Title

Up-regulation of Histone Methyltransferase, DOT1L, by Matrix Hyaluronan Promotes MicroRNA-10 Expression Leading to Tumor Cell Invasion and Chemoresistance in Cancer Stem Cells from Head and Neck Squamous Cell Carcinoma*

Journal

Journal of Biological Chemistry, 291(20)

ISSN

0021-9258

Authors

Bourguignon, Lilly YW
Wong, Gabriel
Shiina, Marisa

Publication Date

2016-05-01

DOI

10.1074/jbc.m115.700021

Peer reviewed

THE JOURNAL OF BIOLOGICAL CHEMISTRY VOL. 291, NO. 20, pp. 10571–10585, May 13, 2016
Published in the U.S.A.

Up-regulation of Histone Methyltransferase, DOT1L, by Matrix Hyaluronan Promotes MicroRNA-10 Expression Leading to Tumor Cell Invasion and Chemoresistance in Cancer Stem Cells from Head and Neck Squamous Cell Carcinoma*

Received for publication, October 21, 2015, and in revised form, March 12, 2016 Published, JBC Papers in Press, March 21, 2016, DOI 10.1074/jbc.M115.700021

Lilly Y. W. Bourguignon[1], **Gabriel Wong, and Marisa Shiina**

From the Endocrine Unit, Department of Medicine, University of California at San Francisco and San Francisco Veterans Affairs Medical Center , San Francisco, California 94121

Human head and neck squamous cell carcinoma is a solid tumor malignancy associated with major morbidity and mortality. In this study, we determined that human head and neck squamous cell carcinoma-derived HSC-3 cells contain a subpopulation of cancer stem cells (CSCs) characterized by a high level of CD44v3 and aldehyde dehydrogenase-1 (ALDH1) expression. Importantly, matrix hyaluronan (HA) induces the up-regulation of stem cell markers that display the hallmark CSC properties. Histone methyltransferase, DOT1L, is also up-regulated by HA in CSCs (isolated from HSC-3 cells). Further analyses indicate that the stimulation of microRNA-10b (miR-10b) expression is DOT1L-specific and HA/CD44-dependent in CSCs. This process subsequently results in the overexpression of RhoGTPases and survival proteins leading to tumor cell invasion and cisplatin resistance. Treatment of CSCs with DOT1L-specific small interfering RNAs (siRNAs) effectively blocks HA/CD44-mediated expression of DOT1L, miR-10b production, and RhoGTPase/survival protein up-regulation as well as reduces tumor cell invasion and enhances chemosensitivity. CSCs were also transfected with a specific anti-miR-10b inhibitor to silence miR-10b expression and block its target functions. Our results demonstrate that the anti-miR-10 inhibitor not only decreases RhoGTPase/survival protein expression and tumor cell invasion, but also increases chemosensitivity in HA-treated CSCs. Taken together, these findings strongly support the contention that histone methyltransferase, DOT1L-associated epigenetic changes induced by HA play pivotal roles in miR-10 production leading to up-regulation of RhoGTPase and survival proteins. All of these events are critically important for the acquisition of cancer stem cell properties, including self-renewal, tumor cell invasion, and chemotherapy resistance in HA/CD44-activated head and neck cancer.

Human head and neck squamous cell carcinoma (HNSCC)[2] is a highly malignant cancer associated with major morbidity and mortality (1). A number of studies have identified specific molecules expressed in HNSCC that correlate with tumor behavior. Among such molecules are matrix hyaluronan (HA) (2, 3) and its cell surface receptor, CD44 (4). HA is a major component of the ECM and is significantly enriched in many types of tumors (5). CD44 is a multifunctional transmembrane glycoprotein expressed in HNSCC cells and carcinoma tissues (6, 7). It is commonly expressed as various isoforms generated by alternative mRNA splicing of variant exons inserted into an extracellular membrane-proximal site (8). Most importantly, expression of certain CD44 variant (CD44v) isoforms (especially, CD44v3) is known to be associated with HNSCC progression (6, 9, 10).

HNSCC appears to contain a subpopulation of cancer stem cells (CSCs) characterized by a high level of CD44v3 expression (10). In fact, CD44v3 is thought to be one of the important cell surface markers for CSCs (10). These isolated CSCs are capable of generating phenotypically distinct cells resulting in heterogeneous tumors in immunodeficient mice. These findings clearly indicate that these CSCs display the hallmark stem cell properties of self-renewal and the ability to generate heterogeneous cell populations. In addition, these CSCs display chemoresistance and thereby can cause recurrence of the cancers (10). However, information regarding CSC-mediated chemotherapy resistance and subsequent HNSCC development is very limited.

MicroRNAs ((miRNAs), small RNA molecules with ~20–25 nucleotides) are closely associated with the pathogenesis of HNSCC (11, 12). In particular, certain miRNAs appear to play a critical role in various CSC functions and tumor progression (9, 10). However, very little is known concerning the regulation of

* This work was supported by Veterans Affairs Merit Review Awards RR and D-1I01 RX000601 and BLR and D-5I01 BX000628, National Institutes of Health Grant R01 CA66163 from USPHS, and a Department of Defense grant. The authors declare that they have no conflicts of interest with the contents of this article. The content is solely the responsibility of the authors and does not necessarily represent the official views of the National Institutes of Health.

[1] Veterans Affairs Senior Research Career Scientist. To whom correspondence should be addressed: San Francisco Medical Center, Dept. of Medicine, University of California at San Francisco, 4150 Clement St., San Francisco, CA 94121. Tel.: 415-221-4810 (Ext. 23321); Fax: 415-383-1638; E-mail: lilly.bourguignon@ucsf.edu.

[2] The abbreviations used are: HNSCC, head and neck squamous cell carcinoma; CSC, cancer stem cell; HA, hyaluronan; ECM, extracellular matrix; APC, allophycocyanin; miRNA, microRNA; IAP, inhibitors of apoptosis; Q-PCR, quantitative PCR; MLL, mixed lineage leukemia; NOD/SCID, non-obese, diabetic/severe combined immunodeficient.

these miRNAs and their function in head and neck cancer. In previous studies, miRNA-10b was found to be overexpressed in malignant glioma in addition to the overexpression of RhoC and urokinase-type plasminogen activator receptor, which are contributors to glioma invasion and migration (13). Moreover, cell invasion and metastasis were both shown to be initiated by miRNA-10b in breast cancer (14). Silencing of miR-10b with antagomirs (an anti-miR-10 inhibitor) both *in vitro* and *in vivo* significantly decreases oncogenesis (15). Thus, the miR-10b inhibitor appears to be a promising candidate for the development of new anti-cancer agents.

Epigenetic changes such as histone methylation have emerged as one of the important regulatory processes in the alteration of chromatin structure and the reprogramming of gene expression during cancer progression (16). Methylation of histone H3 at lysine 79 (H3K79) is highly conserved among most eukaryotic species. In budding yeast, nearly 90% of histone H3 displays either monomethylation (H3K79me1), dimethylation (H3K79me2), or trimethylation (H3K79me3) at lysine 79, all catalyzed exclusively by the histone methyltransferase, DOT1 (17, 18). DOT1 was initially identified as a disruptor of telomeric silencing in *Saccharomyces cerevisiae,* and its orthologs are evolutionarily conserved from yeast to mammals (17, 18). Both DOT1 and the mammalian DOT1L (DOT1-like protein) function as H3K79 methyltransferases in the regulation of histone H3K79 methylation and transcriptional activation (19). In particular, DOT1/DOT1L-mediated H3K79 methylation is known to be involved in the control of transcriptional activity required for cell cycle, meiotic checkpoint, and the DNA damage checkpoint (20). It has also been reported that aberrant H3K79 methylation by DOT1L occurs in mixed lineage leukemia (MLL) (21). Furthermore, down-regulation of DOT1L results in the inhibition of lung cancer cell proliferation (22). These findings all suggest that DOT1L plays an important role in cancer development. An earlier study also indicated that mammalian DOT1L participates in proliferation and differentiation in embryonic stem (ES) cells (23). The question of whether DOT1L-associated H3K79 methylation is involved in HA-mediated CSC signaling and functions in head and neck cancer has not been previously addressed and therefore is the focus of this investigation.

In this study, we report that there is epigenetic regulation induced by DOT1L-mediated H3K79 methylation in HA-activated HNSCC cancer stem cells. Specifically, our results indicate that HA promotes DOT1L-regulated H3K79 methylation leading to miR-10 production, tumor cell invasion, survival, and cisplatin chemoresistance in the CSCs from HNSCC.

Experimental Procedures

Cell Culture—Tumor-derived HSC-3 cell line (isolated from human squamous carcinoma cells of the mouth) was grown in RPMI 1640 medium supplemented with 10% fetal bovine serum.

Antibodies and Reagents—Monoclonal rat anti-CD44 antibody (clone, 020; isotype, IgG_{2b}; obtained from CMB-TECH, Inc., San Francisco) recognizes a determinant of the HA-binding region common to CD44 and its principal variant isoforms such as CD44v3. This rat anti-CD44 was routinely used for HA-related blocking experiments and immunoprecipitation. Other immunoreagents such as rabbit anti-RhoC antibody, rabbit anti-Oct4 antibody, rabbit anti-Nanog antibody, rabbit anti-Sox2 antibody, and goat anti-actin antibody were obtained from R & D Systems (Minneapolis, MN). Mouse anti-cIAP-2 antibody and mouse anti-XIAP antibody were purchased from BD Biosciences. Rabbit anti-monomethyl-H3K79 antibody and mouse anti-DOT1L antibody were from Abcam (Cambridge, MA). Rabbit anti-CD44v3 antibody was obtained from EMD Chemicals (Gibbstown, NJ). Cisplatin was obtained from Sigma. The preparation of HA (~500,000–700,000-dalton polymers) used in these experiments was described previously (9, 10).

Sorting Tumor-derived HSC-3 Cell Populations by Multicolor Fluorescence-activated Cell Sorter (FACS)—The identification of aldehyde dehydrogenase-1 (ALDH1) activity from tumor-derived HSC-3 cells was conducted using the ALDEFLUOR kit (StemCell Technologies, Durham, NC). Specifically, tumor cells were suspended in ALDEFLUOR assay buffer containing ALDH1 substrate (BAAA, 1 mol/liter per 1×10^6 cells) and incubated for 30 min at 37 °C. As a negative control, HSC-3 cells were treated with a specific ALDH1 inhibitor, 50 mmol/liter diethylaminobenzaldehyde (50 mmol/liter).

Next, for labeling the cell surface marker, tumor-derived HSC-3 cells were suspended in 100 μl of ALDEFLUOR buffer followed by incubating with 20 μl of allophycocyanin (APC)-labeled anti-CD44v3 antibody (recognizing the v3-specifc domain of CD44) or APC-labeled normal mouse IgG (as a control) (BD Biosciences) for 15 min at 4 °C. For FACS sorting, tumor cells were suspended in PBS buffer followed by FACS (BD FACSAria IIu) sorting using dual wavelength analysis (10). Routinely, we obtained 5.0×10^6 of $CD44v3^{high}ALDH1^{high}$ cells from 2.5 to 3.0×10^7 tumor-derived HSC-3 cells. Subsequently, $CD44v3^{high}ALDH1^{high}$ tumor cell population was collected and used for various experiments described in this study. Approximately 5×10^5 cells were used during each silencing experiment described in the text.

Tumorigenicity Assay—Non-obese, diabetic/severe combined immunodeficient (NOD/SCID) immunocompromised mice (5-week-old female mice) were purchased from Charles River Laboratories International, Inc. (Wilmington, MA), and maintained in micro-isolator cages. Specifically, these NOD/SCID mice were injected subcutaneously and/or submucosally in the floor of the mouth with sorted $CD44v3^{high}ALDH1^{high}$ cells or unsorted HSC-3 cells (suspended in 0.1 ml of Matrigel Basement Membrane Matrix) ranging from 50, 500, to 5,000 cells as described previously (10). These mice were then monitored twice weekly for palpable tumor formation and euthanized 4 or 8 weeks after transplantation to assess tumor formation. Tumors were measured using a Vernier caliper, weighed, and photographed. A portion of the subcutaneous tumors and/or submucosa tumors was collected. Some tumors were cut into small fragments with sterile scissors and minced with a sterile scalpel, rinsed with Hanks' balanced salt solution containing 2% heat-inactivated calf serum (Invitrogen), and centrifuged for 5 min at 1,000 rpm. The resulting tissue specimen was placed in a solution of DMEM/F-12 containing 300 units/ml collagenase and 100 units/ml hyaluronidase (StemCell Tech-

nologies, Durham, NC). The mixture was incubated at 37 °C to dissociate cells. The digestion was arrested with the addition of FBS, and the cells were filtered through a 40-μm nylon sieve. The cells were washed twice with Hanks' balanced salt solution plus 2% heat-inactivated calf serum for FACS as described above.

Immunoblotting Techniques—First, $CD44v3^{high}ALDH1^{high}$ cells (untransfected cells with normal IgG (10 μg/ml) or anti-CD44 antibody (10 μg/ml) treatment or transfected cells with DOT1L siRNA or siRNA with scrambled sequences; or anti-miR-10b inhibitor or miRNA-negative control treatment followed by HA (50 μg/ml) or no HA addition for 24 h) were solubilized in a lysis buffer containing 0.5% Nonidet P-40 and various protease inhibitors followed by immunoblotting with various immunoreagents such as anti-Oct4 antibody (2 μg/ml) or anti-Sox2 antibody (2 μg/ml) or anti-Nanog antibody (2 μg/ml) or anti-DOT1L (2 μg/ml) or anti-monomethyl-H3K79 (2 μg/ml) or anti-RhoC (2 μg/ml) or anti-cIAP-2 (2 μg/ml) and anti-XIAP (2 μg/ml) or anti-actin (2 μg/ml) (as a loading control), respectively.

Chromatin Immunoprecipitation (ChIP) Assay—To examine whether H3K79 methylation directly interacts with the E-box region of miR-10b promoter, chromatin immunoprecipitation (ChIP) assays was performed in $CD44v3^{high}ALDH1^{high}$ cells (untransfected cells with normal IgG (10 μg/ml) or anti-CD44 antibody (10 μg/ml) treatment or transfected with DOT1L siRNA or siRNA with scrambled sequences, followed by 1 h of HA (50 μg/ml) or no HA addition) using a kit (EZ ChIP) from Millipore Corp. according to the manufacturer's instructions. DNA fragments were then extracted with a PCR purification kit and analyzed by PCR or quantitative PCR (Q-PCR) using primer pairs 5′-ACCTGGCTTGGTCGGGCAGT-3′ and 5′-CGCAGCCACCCGCACTTTCT-3′. These primers gave a single strong band when tested on input DNA on an agarose gel.

Q-PCR—Total RNA was isolated from $CD44v3^{high}ALDH1^{high}$ cells (untransfected cells with rat anti-CD44 (10 μg/ml) or normal rat IgG (10 μg/ml) or transfected with DOT1LsiRNA (30 nM) or siRNA with scrambled sequences (30 nM); or anti-miR-10b inhibitor (30 nM) or miRNA-negative control (30 nM) followed by HA (50 μg/ml) or no HA addition for 24 h) using Tripure Isolation Reagent kits (Roche Applied Science). First-stranded cDNAs were synthesized from RNA using Superscript first-strand synthesis system (Invitrogen). Gene expression was quantified using probe-based SYBR Green PCR master mix kits, ABI PRISM 7900HT sequence detection system, and SDS software (Applied Biosystems, Foster City, CA). A cycle threshold (minimal PCR cycles required for generating a fluorescent signal exceeding a preset threshold) was determined for each gene of interest and normalized to a cycle threshold for a housekeeping gene (36B4) determined in parallel. The 36B4 is a human acidic ribosomal phosphoprotein PO whose expression was not changed in tumor cells. The Q-PCR primers used for detecting miR-10b expression was as follows: specifically, two miR-10b-specific primers (the sense primer 5′-GGATACCCTGTAGAACCGAA and the antisense primer 5′-CAGTGCGTGTCGTGGAGT) were used. Finally, for detecting 36B4 gene expression, two 36B4-specific primers (the sense primer 5′-GCGACCTGGAAGTCCAACTAC-3′ and the antisense primer 5′-ATCTGCTGCATCTGCTTGG-3′) were used.

Transfection Experiments—miR-10b inhibitor, miRNA-negative control, various siRNAs targeting DOT1L, RhoC, cIAP-2, XIAP, and scrambled sequenced siRNAs (negative control siRNAs) were purchased from Ambion (Foster City, CA). $CD44v3^{high}ALDH1^{high}$ cells were then transfected with various reagents (described above) using Lipofectamine 2000 reagent (Invitrogen) for 24 h. The final concentrations of anti-miR-10b inhibitor, miRNA-negative control, various siRNAs, and silencer negative control siRNAs used in various experiments were 30 nM. Cells were then treated with HA or without HA in various experiments as described below.

Clinical Tumor Samples—IRB approval was obtained from our institution's Committee on Human Research. The clinical tissue specimens were portions of primary tumors of patients undergoing surgical treatment of HNSCC from multiple primary sites of the upper aerodigestive tract at the University of California at San Francisco-affiliated Veterans Affairs Medical Center from September 1, 2001, to June 30, 2006. The presence of ≥80% cancer cells in the procured samples was confirmed by a clinical pathologist.

Immunohistochemistry Staining—Human HNSCC patient tissue specimens were fixed in 4% formaldehyde in 0.1 M phosphate buffer for 24 h at 4 °C and embedded in paraffin. Immunohistochemical stains using rabbit anti-CD44v3 antibody or rabbit anti-DOT1L antibody were performed using the Vectastain ABC kit (Vector Laboratories, Burlingame, CA), according to the manufacturer's protocol.

Tumor Cell Growth Assays—To analyze growth properties, these sphere-derived $CD44v3^{high}ALDH1^{high}$ cells (untransfected cells with rat anti-CD44 (10 μg/ml) or normal rat IgG (10 μg/ml), or transfected with DOT1LsiRNA or RhoCsiRNA or cIAP-2siRNA or XIPAsiRNA, or scrambled sequenced siRNA, or pretreated with anti-miR-10b inhibitor or miRNA-negative control) were also incubated with various concentrations of cisplatin (4×10^{-9} to 1.75×10^{-5} M) in the presence or absence of HA (50 μg/ml). After 24 h of incubation at 37 °C, growth assays were analyzed using the 3-(4,5-dimethylthiazol-2-yl)-2,5-diphenyltetrazolium bromide assay. Specifically, 50% inhibitory concentration (IC_{50}) was identified as a concentration of drug required to achieve a 50% growth inhibition relative to untreated controls as described previously (10).

Tumor Cell Invasion Assay—Twenty four transwell units were used for monitoring *in vitro* tumor cell invasion using $CD44v3^{high}ALDH1^{high}$ (untransfected cells with rat anti-CD44 (10 μg/ml) or normal rat IgG (10 μg/ml) or transfected with DOT1LsiRNA or RhoCsiRNA or cIAP-2siRNA or XIPAsiRNA or siRNA with scrambled sequences; or anti-miR-10b inhibitor or miRNA-negative control) followed by HA (50 μg/ml) treatment for 24 h as described previously (15).

Results

Isolation of a Highly Tumorigenic Cell Population from Tumor-derived HNSCC Cells Using FACS

Overexpression of CD44v3 has been shown to be closely associated with HNSCC development and progression. ALDH1,

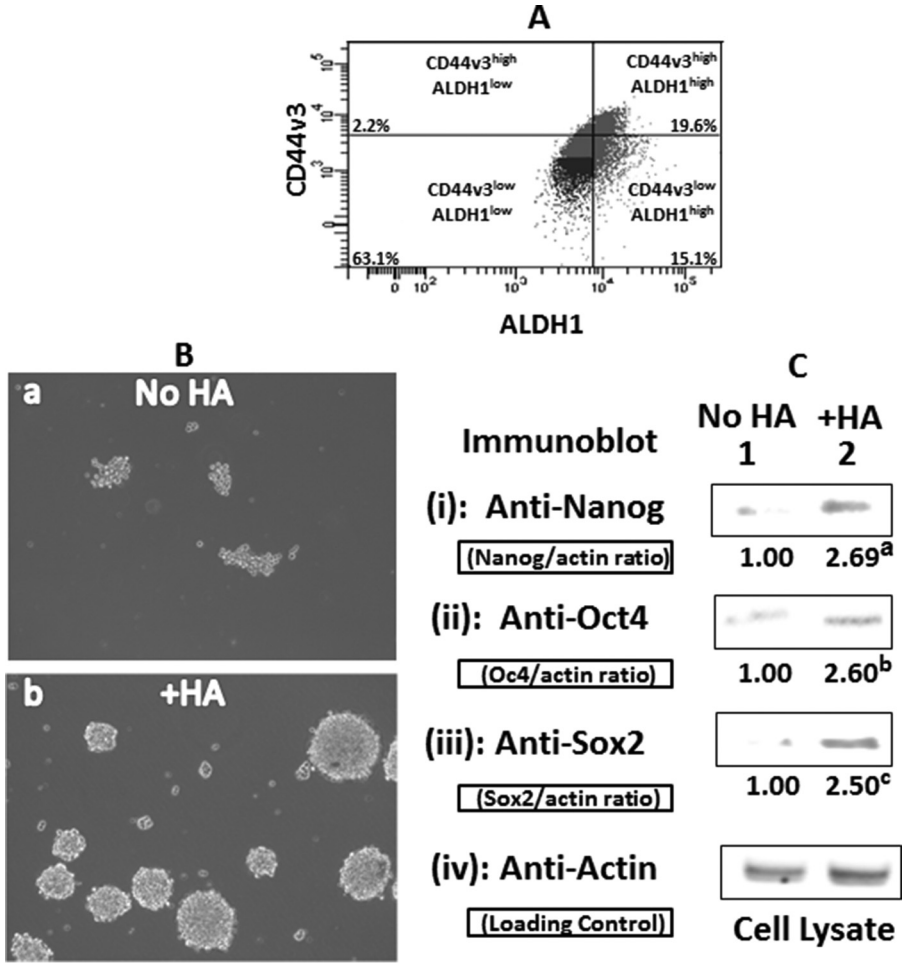

FIGURE 1. **Isolation of cancer stem cell-like population from tumor-derived HNSCC (HSC-3 cells) using multicolor FACS.** Tumor-derived human HNSCC (HSC-3 cells) were incubated with both ALDEFLUOR kit (to measure an ALDH1 enzymatic activity) and APC-labeled anti-CD44v3 antibody (recognizing the v3-specific domain of CD44) followed by FACS and cell sorting (*A*). *A,* flow cytometry analyses of HSC-3 tumor cell populations, including $CD44v3^{high}ALDH1^{high}$ (*top right quad*, 19.6%) or $CD44v3^{high}ALDH1^{low}$, (*top left quad*, 2.2%) or $CD44v3^{low}ALDH1^{high}$ (*bottom right quad*, 15.1%) or $CD44v3^{low}ALDH1^{1ow}$ (*bottom left quad*, 63.1%). Live tumor cell sorting was then done using a FACS to isolate $CD44v3^{high}ALDH1^{high}$ cells or $CD44v3^{low}ALDH^{1ow}$ for the study. *B,* measurement of sphere formation by incubating $CD44v3^{high}ALDH1^{high}$ cells (treated with no HA (*panel a*) or with HA (*panel b*)) in serum-free RPMI 1640 medium (containing EGF and bFGF) for 3 weeks (21-days) as described under "Experimental Procedures." *C,* detection of stem cell marker expression in $CD44v3^{high}ALDH1^{high}$ cells treated with no HA (*lane 1*) or with HA (*lane 2*). The expression of stem cell markers such as Nanog, Oct4, and Sox2 was measured using anti-Nanog antibody (*i*) or anti-Oct4 (*ii*) or anti-Sox2 (*iii*) or anti-actin (loading control) (*iv*) according to the procedures described under the "Experimental Procedures." (The ratio of Nanog (*i*) or Oct 4 (*ii*) or Sox2 (*iii*) and actin (*iv*) was determined by densitometry and normalized to the value of control (no HA-treated samples) designated as 1:00. The values expressed represent an average of triplicate determination of four experiments with S.D. of less than 5%.) ^{a,b,c}, statistically significant ($p < 0.005$; analysis of variance; $n = 4$) as compared with control samples (no HA addition).

a detoxifying enzyme responsible for the oxidation of intracellular aldehydes, is also considered to be a common marker for both normal stem cells and malignant CSCs from HNSCC (10, 24, 25). Overexpression of both CD44v3 and ALDH1 appears to be closely associated with CSC-mediated HNSCC development and progression (10). In this study we utilized the ALDEFLUOR kit (to detect an ALDH1 enzymatic activity) (Fig. 1*A*) and APC-labeled anti-CD44v3 antibody (recognizing the v3-specifc domain of CD44) (Fig. 1*A*) followed by FACS analysis to identify four tumor cell populations as follows: (i) $CD44v3^{high}ALDH1^{high}$; (ii) $CD44v3^{high}ALDH1^{low}$; (iii) $CD44v3^{low}ALDH1^{high}$; and (iv) $CD44v3^{low}ALDH1^{1ow}$. $CD44v3^{high}ALDH1^{high}$, $CD44v3^{low}ALDH1^{high}$, and $CD44v3^{low}ALDH1^{1ow}$ represented 19.6, 15.1, and 63.1% of total tumor cell population, respectively, as the three major cell populations.

$CD44v3^{high}ALDH1^{low}$ (Fig. 1*A*, representing 2.2%) is present as a very minor tumor cell population. Subsequently, we employed a FACS to isolate the three major tumor cell populations as follows: $CD44v3^{high}ALDH1^{high}$, $CD44v3^{low}ALDH1^{high}$, and $CD44v3^{low}ALDH1^{1ow}$ cells. We then found that $CD44v3^{high}ALDH1^{high}$ cells were capable of forming large tumors in NOD/SCID immunocompromised mice injected with as few as 50 $CD44v3^{high}ALDH1^{high}$ cells (Table 1). These results indicate that the $CD44v3^{high}ALDH1^{high}$ cells (to a much lesser extent $CD44v3^{low}ALDH1^{high}$ or $CD44v3^{low}ALDH1^{1ow}$ cells or unsorted cells) are very tumorigenic and strongly suggest that the $CD44v3^{high}ALDH1^{high}$ cell population displays CSC-like properties. Further analysis indicates that the $CD44v3^{high}ALDH1^{high}$ cells are capable of growing and forming large spheres in serum-free defined medium for more than 21 days (Fig. 1*B* and Table 2). These cells also express stem cell markers (*e.g.* Nanog, Oct4, and Sox2) (Fig. 1*C*). In the presence of HA, both cell growth and the size of the spheres formed are greatly increased (Fig. 1, *B, panel b,* and *C, lane 2,* and Table 2),

TABLE 1
Analyses of tumor formation by CD44v3^{high}ALDH1^{high} cells, CD44v3^{low}ALDH1^{low} cells, CD44v3^{low}ALDH1^{high} cells, or unsorted cells subcutaneously injected into NOD/SCID mice

Cell populations	Tumor formation[a]		
	5,000 cells injected (8 weeks)	500 cells injected (8 weeks)	50 cells injected (8 weeks)
CD44v3^{high}ALDH1^{high} cells	20/20	18/20	16/20
CD44v3^{low}ALDH1^{high} cells	3/20	1/20	0/20
CD44v3^{low}ALDH1^{low} cells	1/20	0/20	0/20
Unsorted cells	2/20	0/20	0/20

[a] For the tumor cell injection, each mouse was subcutaneously inoculated with CD44v3^{high}ALDH1^{high} cells or CD44v3^{low}ALDH1^{high} cells or CD44v3^{low}ALDH1^{low} cells or unsorted cells with 5,000 cells, 500 cells, or 50 cells as described under "Experimental Procedures." The values expressed in the table represent the number of animals that developed tumors/total number of animals used in the study. The tumor formation assay was performed on at least five different experiments with a standard deviation less than ±5%.

TABLE 2
Measurement of sphere formation and self-renewal/growth using CD44v3^{high}ALDH1^{high} cells

(A) **Effects of HA on sphere formation of CD44v3^{high}ALDH1^{high} cells.**

Treatments	1st Generation Sphere Formation (SFU)[a] (% of control)*	2nd Generation Sphere Formation (SFU)[a] (% of control)*	3rd Generation Sphere Formation (SFU)[a] (% of control)*
No HA treatment (control)	100 ± 7	100 ± 5	100 ± 6
HA treatment	180 ± 10	209 ± 14	220 ± 18

(B) **Effects of HA on CD44v3^{high}ALDH^{high} cell growth:**

Treatments	Tumor Cell Growth[b] (Cells dissociated from 1st Generation Spheres) (% of control)*	Tumor Cell Growth[b] (Cells dissociated from 2nd Generation Spheres) (% of control)*	Tumor Cell Growth[b] (Cells dissociated from 3rd Generation Spheres) (% of control)*
No HA treatment (control)	100 ± 7	100 ± 5	100 ± 6
HA treatment	192 ± 9	210 ± 12	230 ± 18

[a] Sphere formation (using CD44v3^{high}ALDH1^{high} cells from the serial passage of 1st, 2nd, and 3rd generation of spheres) was measured by sphere formation unit (SFU) as described under "Experimental Procedures." The sphere formation in cells treated with no HA (Table 3, A, control) is designated as 100%.
[b] Measurement of growth for CD44v3^{high}ALDH1^{high} cells (dissociated from spheres after a serial passage of 1st, 2nd, and 3rd generation of sphere formation) was performed by incubating these cells in serum-free RPMI 1640 medium for 3 weeks (21 days) using 3-(4,5-dimethylthiazol-2-yl)-2,5-diphenyltetrazolium bromide-based growth assay as described under "Experimental Procedures." Tumor cell growth in cells treated with no HA (Table III, B, control) is designated as 100%.

and the level of all three stem cell marker expressions is also enhanced (at least ~2.50-fold increase) (Fig. 1*C, lane 2*) as compared with various properties (*e.g.* tumor cell growth, size of sphere formation, and stem cell marker expression) detected in CD44v3^{high}ALDH1^{high} cells treated with no HA (Fig. 1, *B, panel a*, *C, lane 1,* and Table 2). These observations indicate that HA induces CSC-like properties (*e.g.* stem cell marker expression and sphere formation) and cell growth/self-renewal (demonstrated by serial passage of sphere-forming ability and long term tumor cell growth) in the highly tumorigenic CD44v3^{high}ALDH1^{high} cells. The cellular mechanism that produces the highly tumorigenic CSC properties of CD44v3^{high}ALDH1^{high} cells was unknown and is therefore the focus of this investigation.

HA-induced Up-regulation of DOT1L and H3K79 Methylation in Tumorigenic CD44v3^{high}ALDH1^{high} (CSC-like) HNSCC Cells

In mammalian cells, several reports have linked DOT1L and monomethyl-H3K79 with active transcription (19). To investi-

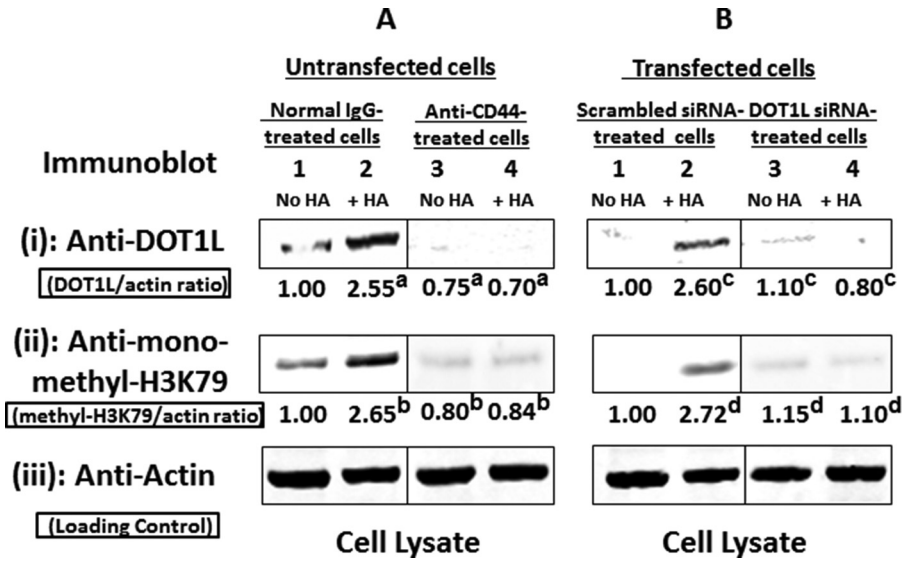

FIGURE 2. **Effects of HA on stimulating DOT1L expression and H3K79 methylation in CD44v3^{high}ALDH1^{high} cells.** Detection of the expression of DOT1L and H3K79 methylation using anti-DOT1L (*panel i*) and anti-monomethyl-H3K79 (*panel ii*)-mediated immunoblotting using cell lysate isolated from CD44v3^{high}ALDH1^{high} cells. *A,* untransfected CD44v3^{high}ALDH1^{high} cells treated with normal IgG (*lanes 1* and *2*) or anti-CD44 antibody (*lanes 3* and *4*) in the absence of HA (*lanes 1* and *3*) or the presence of HA (lanes 2 and 4) for 24 h. *B*, CD44v3^{high}ALDH1^{high} cells transfected with scrambled siRNA with no HA (*lane 1*) or with HA (*lane 2*) for 24 h. CD44v3^{high}ALDH1^{high} cells transfected with DOT1L siRNA with no HA (*lane 1*) or with HA (*lane 2*) for 24 h. (Anti-actin-mediated immunoblot is used as a loading control (*d*).) (The ratio of DOT1L (*panel i*) or monomethyl-H3K79 (*panel ii*), and actin (*panel iii*) was determined by densitometry and normalized to the value of control (untransfected cells-normal IgG or scrambled siRNA) with no HA-treated samples) designated as 1:00. The values expressed represent an average of triplicate determination of four experiments with S.D. of less than 5%.) ^{a,b}, statistically significant ($p < 0.001$; analysis of variance; $n = 4$) as compared with control samples (normal IgG-treated cells without HA addition); ^{c,d}, statistically significant ($p < 0.001$; analysis of variance; $n = 4$) as compared with control samples (scrambled siRNA-treated cells without HA addition).

gate whether the expression of DOT1L-associated H3K79 methylation occurs in CD44v3^{high}ALDH1^{high} (CSC-like) cells, we performed an anti-DOT1L or anti-monomethyl-H3K79-mediated immunoblots. Our results indicate that the expression of both DOT1L and monomethyl-H3K79 is significantly enhanced (at least ~2.50-fold up-regulation) in untransfected CD44v3^{high}ALDH1^{high} cells (treated with normal IgG) in the presence of HA (Fig. 2*A, i* and *ii, lane 2*) as compared with those DOT1L or monomethyl-H3K79 present in untransfected cells (treated with normal IgG) in the absence of HA (Fig. 2, *A, i* and *ii, lane 1*) or treated with anti-CD44 antibody in the presence or absence of HA (Fig. 2, *A, i* and *ii, lanes 3* and *4*). These findings establish the notion that the up-regulation of DOT1L and H3K79 methylation in untransfected CD44v3^{high}ALDH1^{high} is HA/CD44-dependent. Further analysis indicates that there is significant reduction of DOT1L and monomethyl-H3K79 expression (at least ~40–70% decrease) detected in CD44v3^{high}ALDH1^{high} (CSC-like) cells treated with DOT1L siRNA (in the presence or absence of HA) as compared with DOT1L and H3K79 methylation detected in scrambled siRNA-treated cells with HA (Fig. 2*B, i* and *ii, lanes 3* and *4 versus lanes 1* and *2*). These results suggest that HA-mediated up-regulation of H3K79 methylation in these CSC-like CD44v3^{high}ALDH1^{high} cells requires DOT1L.

Our immunostaining data indicate that both CD44v3 (using anti-CD44v3-mediated staining, Fig. 3*B*) and DOT1L (using anti-DOT1L-mediated staining, Fig. 3*C*) (but not normal IgG-mediated staining) can be detected in human HNSCC samples (indicated by H&E staining, Fig. 3*A*). These findings support the contention that overexpression of CD44v3 and DOT1L is closely associated with HNSCC patient samples.

Binding of DOT1L-associated Monomethyl-H3K79 to E-box Elements in the miR-10b Promoter Leading to miR-10b Production in HA-treated CD44v3^{high}iALDH1^{high} Cells

The expression of miR-10b has been shown to be involved in CSCs (26). Several predicted E-box elements are located upstream of miR-10b (14), which is a class of miRNA known to be associated with tumor cell invasion and metastasis. To examine whether DOT1L-activated H3K79 methylation (in particular, monomethyl-H3K79) directly interacts with the E-box elements in the promoter region of miR-10b, anti-monomethyl-H3K79 antibody-specific chromatin immunoprecipitation (ChIP) assays were performed in CD44v3^{high}ALDH1^{high} cells. As shown in Fig. 4*A*, PCR results from anti-monomethyl-H3K79-mediated precipitations from HA-treated CD44v3^{high}ALDH1^{high} cells identify a specific amplification product using a primer pair specific for the miR-10b promoter region (containing the monomethyl-H3K79 binding sites in scrambled siRNA-treated (Fig. 4*A*, *panel I, a*, *lane 2*) or normal IgG-treated (Fig. 4 *A, panel II, a, lane 4*) CD44v3^{high}ALDH1^{high} cells following HA addition. In contrast, a significantly reduced amount of monomethyl-H3K79-mediated binding of the miR-10b promoter region was found in these cells treated with no HA (Fig. 4, *A, panel I, a, lane 1*, and *panel II, a, lane 3*). The fact that pretreatment of cells with DOT1L siRNA (Fig. 4*A, panel I, a, lane 4 versus lane 3*) or anti-CD44 antibody (Fig. 4*A, panel II, a, lane 2 versus lane 1*) followed by HA (or no HA) addition significantly reduces the ability of monomethyl-H3K79 binding to the promoter of miR-10b. These findings suggest that the monomethyl-H3K79 signaling event transcriptionally activates miR-10b promoter activity in CD44v3^{high}ALDH1^{high} cells in a

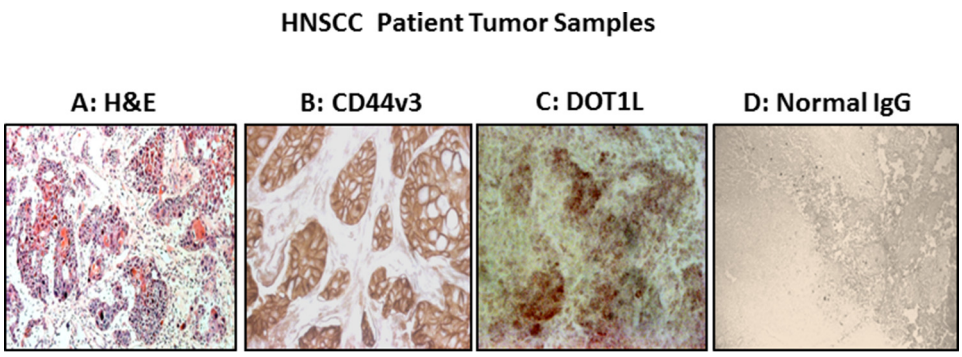

FIGURE 3. **Detection of CD44v3 and DOT1L expression in human HNSCC patient samples.** A panel of immunoreagents, including anti-CD44v3 antibody and anti-DOT1L antibody, was used to examine the expression of CD44v3 and DOT1L in human HNSCC patient tumors. H&E staining (*A*), immunoperoxidase staining of CD44v3 (*B*), DOT1L, (*C*), and normal IgG (*D*) using HNSCC patient tumor samples.

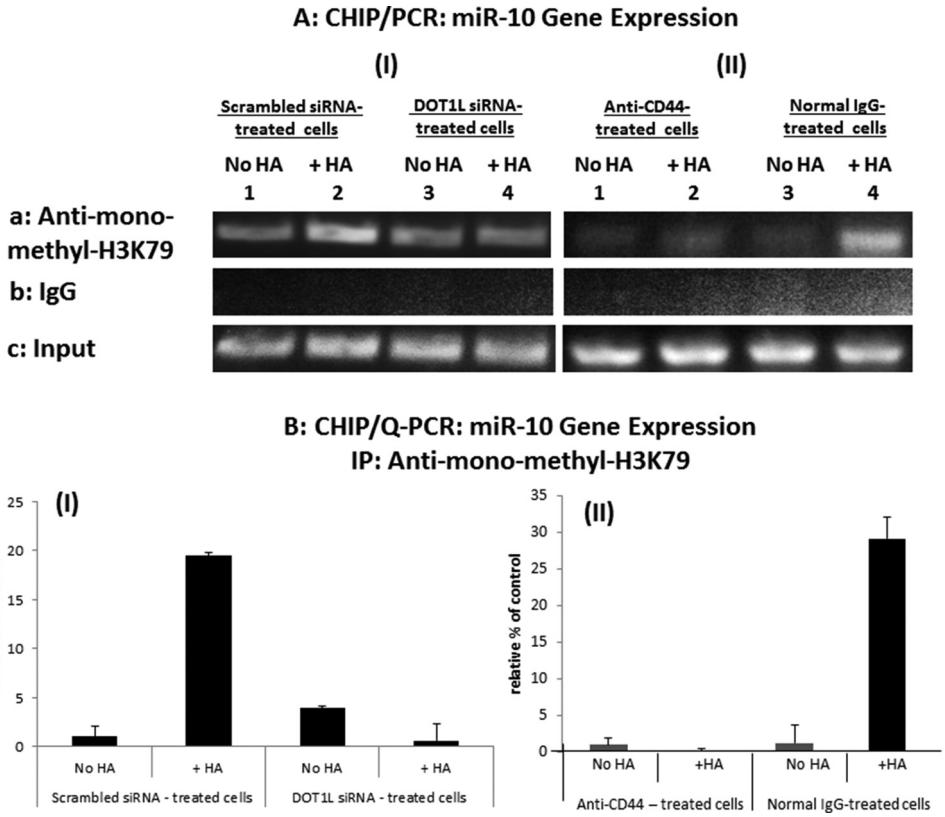

FIGURE 4. **Interaction between monomethyl-H3K79 and the miR-10b promoter in CD44v3^{high}ALDH1^{high} cells.** *A,* ChIP assay was performed in CD44v3^{high}ALDH1^{high} cells using monomethyl-H3K79 binding site containing miR-10b promoter-specific primers and PCR analyses. Identical volumes from the final precipitated materials (anti-monomethyl-H3K79 immunoprecipitated material (*a*); or IgG isotype control-precipitated materials (*b*); or total input materials (*c*)) were used. *Panel I*, cells treated with scrambled (*SC*) siRNA with no HA (*lane 1*) or with 1 h of HA treatment (*lane 2*); cells transfected with DOT1L siRNA with no HA (*lane 3*) or with 1 h of HA treatment (*lane 4*). *Panel II*, cells treated with anti-CD44 antibody with no HA (*lane 1*) or with 1 h HA treatment (*lane 2*); and cells treated with normal IgG with no HA (*lane 3*) or with 1 h of HA treatment (*lane 4*) were used. *B,* ChIP assay was also performed in CD44v3^{high}ALDH1^{high} cells using monomethyl-H3K79 binding site-containing miR-10b promoter-specific primers and Q-PCR analyses. Identical volumes from the final precipitated materials (anti-monomethyl-H3K79 immunoprecipitated (*IP*) material (*a*), or IgG isotype control-precipitated materials (*b*), or total input materials (*c*), as described above)) were used. *Panel I*, cells were treated with scrambled (*SC*) siRNA with no HA or with 1 h of HA treatment; cells were treated with DOT1L siRNA with no HA addition or with 1 h of HA treatment. *Panel II,* cells were treated with anti-CD44 antibody with no HA or with 1 h of HA treatment, or cells were treated with normal IgG with no HA or with 1 h of HA treatment. The values expressed in this figure represent an average of triplicate determinations of 3–5 experiments with a standard deviation less than ±5%.

CD44 and DOT1L-dependent manner. Identical amplification products were detected in the positive controls from total input chromatin (Fig. 4, *A, panel I, c, lanes 1–4,* and *A, panel II, c, lanes 1–4*). Moreover, no amplification was seen in samples that were processed in IgG isotype control-mediated precipitation (Fig. 4, *A, panel I, b, lanes 1–4,* and *A, panel II, b, lanes 1–4*). We also observed very similar results by Q-PCR (Fig. 4*B, panels I* and *II*).

In addition, our results indicate that the level of miR-10b is increased in CD44v3^{high}ALDH1^{high} cells treated with scrambled sequence siRNA or normal IgG plus HA compared with those cells without HA addition (Fig. 5, *A* and *C*). CD44v3^{high}ALDH1^{high} cells treated with DOT1L siRNA (Fig. 5*A*) or anti-CD44 antibody (Fig. 5*C*) show significantly less HA-induced miR-10b expression. Moreover, we have found that the expression of miR-10b can be induced in cells treated with an

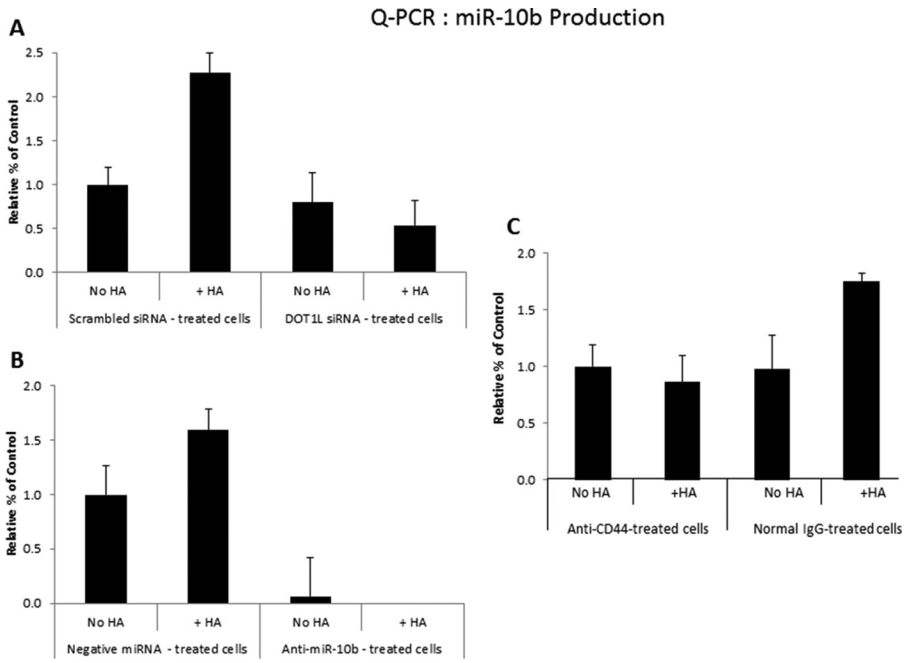

FIGURE 5. **Detection of HA-induced miR-10b production in CD44v3^{high}ALDH1^{high} cells.** Detection of miR-10b production in CD44v3^{high}ALDH^{high} cells using Q-PCR analyses was described under "Experimental Procedures." *A,* detection of miR-10b expression in CD44v3^{high}ALDH1^{high} cells incubated with scrambled (*SC*) siRNA with no HA treatment or with 6 h of HA treatment or transfected with DOT1L siRNA with no HA treatment or with 6 h of HA treatment. *B,* detection of miR-10b expression in CD44v3^{high}ALDH1^{high} cells incubated with negative miRNA control with no HA treatment or with 6 h of HA treatment or pretreated with an anti-miR-10b inhibitor with no HA treatment or with 6 h of HA treatment. *C,* detection of miR-10b expression in CD44v3^{high}ALDH1^{high} cells incubated with anti-CD44 antibody with no HA treatment or with 6 h of HA treatment or treated with normal IgG with no HA treatment or with 6 h of HA treatment. (The optimal time point for the induction of miR-10 occurs at 6 h of HA incubation. Therefore, cells treated with HA for 6 h were used for the study. Values expressed in this figure represent an average of triplicate determinations of 3–5 experiments with a standard deviation less than ±5%.)

miRNA negative control upon addition of HA (Fig. 5*B*). In contrast, the treatment of CD44v3^{high}ALDH1^{high} cells with an anti-miR-10b inhibitor plus HA results in a decrease in miR-10b expression (Fig. 5*B*). These results suggest that HA-induced monomethyl-H3K79 binding to the promoter region of miR-10b and the subsequent miR-10 production require both CD44 and DOT1L in CD44v3^{high}ALDH1^{high} cells.

DOT1L-H3K79-associated miR-10b Signaling in Regulating HA-mediated Invasion and Chemoresistance in CD44v3^{high}ALDH1^{high} Cells

In this part of the study, we have observed that HA enhances tumor cell invasion (at least ~2.5-fold increase) (Table 3, A) and decreases the ability of cisplatin to induce apoptosis and cell death of these CD44v3^{high}ALDH1^{high} cells (in the presence of normal IgG) leading to the enhancement of chemoresistance (at least ~2.5-fold increase in cisplatin-resistance) (Table 4, A) as compared with those cells treated with no HA. In contrast, when CD44v3^{high}ALDH1^{high} cells were treated with anti-CD44 antibody (in the presence or absence of HA), they appear to become less invasive (at least 40–70% reduction in invasiveness) (Table 3, A) and more sensitive to cisplatin-induced apoptosis and cell death (at least ~40–90% reduction in cisplatin resistance) (Table 4, A) as compared with those cells treated with normal IgG plus HA. These findings suggest that HA-mediated cell invasion and cisplatin resistance in these CSC-like CD44v3^{high}ALDH1^{high} cells are CD44-dependent.

Previous studies indicated that miR-10b may function as an oncogene and play a role in promoting tumor cell invasion and chemoresistance, in part through up-regulation of cytoskeleton regulators (14, 15). However, identification of miR-10b-specific downstream target(s) and oncogenic event(s) that contribute to HA/CD44-dependent CD44v3^{high}ALDH1^{high} cell invasion, survival, and chemoresistance has not been determined.

Cytoskeleton Regulators as the Possible Target(s) for DOT1L-H3K79 Methylation-associated miR-10b Signaling Pathway in Regulating CD44v3^{high}ALDH1^{high} Cell Invasion—Previous studies indicated that miR-10b plays a role in promoting tumor cell invasion, in part through up-regulation of RhoGTPases (13–15). To determine how cellular changes regulated by miR-10b (via HA signaling) may affect CD44v3^{high}ALDH1^{high} cell-specific behaviors (*e.g.* tumor cell invasion), we analyzed the expression of the cytoskeleton regulator, RhoGTPase (RhoC). Immunoblot analyses using anti-RhoC antibody were employed to detect the production of the RhoGTPase, RhoC, in CD44v3^{high}ALDH1^{high} cells. Our data indicate that HA significantly stimulates RhoC expression (at least ~2.5-fold increase) followed by an enhanced level of tumor cell invasion (at least ~2.5-fold increase) in CD44v3^{high}ALDH1^{high} cells (incubated with an miRNA-negative control reagent or scrambled sequence siRNA) (Fig. 6, *A* and *B* (*panel i*), *lane 2,* and Table 3, B) as compared with the amount of RhoC expression and the extent of tumor invasion in those CD44v3^{high}ALDH1^{high} cells (treated with a miRNA-negative control reagent or scrambled sequence siRNA) in the absence of HA (Fig. 6, *A* and *B* (*panel i*),

TABLE 3
Measurement of HA-mediated CD44v3^{high}ALDH1^{high} cell invasion

(A) Effects of CD44 antibody on HA-mediated CD44v3^{high}ALDH^{high} cell invasion:

Treatments	Tumor Cell Invasion* (% of control)**	
	Normal IgG-treated cells	Anti-CD44-treated cells
No treatment (control)	100 ± 3	78 ± 2[a]
HA treatment	255 ± 10[a]	75 ± 2[a]

(B) Effects of DOT1LsiRNA on HA-mediated CD44v3^{high}ALDH^{high} cell invasion:

Treatments	Tumor Cell Invasion* (% of control)**	
	Scrambled siRNA-treated cells	DOT1L siRNA-treated cells
No treatment (control)	100 ± 2	88 ± 3[b]
HA treatment	250 ± 8[b]	80 ± 4[b]

(C) Effects of anti-miR-10b inhibitor on HA-mediated CD44v3^{high}ALDH1^{high} cell invasion:

Treatments	Tumor Cell Invasion* (% of control)**	
	Negative miRNA-treated cells	Anti-miR-10b inhibitor-treated cells
No treatment (control)	100 ± 4	85 ± 2[c]
HA treatment	254 ± 10[c]	82 ± 3[c]

(D) Effects of RhoC siRNA, cIAP-2siRNA & XIAP siRNA on HA-mediated CD44v3^{high}ALDH1^{high} cell invasion:

Treatments	Tumor Cell Invasion* (% of control)**			
	Scrambled siRNA-treated cells	RhoC siRNA-treated cells	cIAP-2 siRNA-treated cells	XIAP siRNA-treated cells
No treatment (control)	100 ± 4	73 ± 3[d]	82 ± 3[d]	80 ± 2[d]
HA treatment	258 ± 5[d]	70 ± 2[d]	85 ± 4[d]	87 ± 3[d]

* Twenty four transwell units containing 5-μm porosity polycarbonate filters coated with the reconstituted basement membrane substance Matrigel were used for monitoring *in vitro* tumor cell invasion. Specifically, CD44v3^{high}ALDH1^{high} cells [1×10^4 cells/well-untransfected (treated with normal IgG or anti-CD44 antibody) or transfected with DOT1L siRNA, RhoC siRNA, cIAP-2 siRNA, XIAP siRNA, or scrambled siRNA or negative miRNA control or anti-miR-10b inhibitor] were placed in the upper chamber of the transwell unit in the presence of 50 μg/ml HA. The growth medium containing high glucose DMEM supplemented by 10% fetal bovine serum were placed in the lower chamber of the transwell unit. After 18h incubation at 37 °C in a humidified 95% air, 5% CO_2 atmosphere, cells on the upper side of the filter were removed by wiping with a cotton swab. Cell invasion processes were determined by measuring the cells that migrated and invaded to the lower side of the polycarbonate filters by standard cell number counting methods. The CD44-specific cell invasion was determined by subtracting non-specific cell invasion [*i.e.* cells that migrated (invaded) to the lower chamber in the presence of anti-CD44 antibody treatment]. The CD44-specific cell invasion in normal IgG/scrambled siRNA-treated cells without HA (A and B and D, control) or negative miRNA-treated cells without HA (C, control) is designated as 100%. The values expressed in this Table are presented as the means ± S.D. All assays consisted of at least six replicates and were performed on at least five different experiments.

[a] Data are statistically significant ($P < 0.005$; analysis of variance; $n = 5$) as compared with control samples (normal IgG-treated cells without HA addition).

[b,d] Data are statistically significant ($P < 0.005$; analysis of variance; $n = 5$) as compared with control samples (scrambled siRNA-treated cells without HA addition).

[c] Data are statistically significant ($P < 0.005$; analysis of variance; $n = 5$) as compared with control samples (miRNA negative control-treated cells without HA addition).

TABLE 4
Measurement of cisplatin-induced CD44v3^{high}ALDH1^{high} cell growth inhibition

(A) Effects of CD44 antibody on cisplatin-induced cell growth inhibition in CD44v3^{high}ALDH1^{high} cells.

Treatments	Cisplatin-Induced Tumor Cell Growth Inhibition IC_{50} (μM)*	
	Normal IgG-treated cells	Anti-CD44-treated cells
No treatment (control)	2.20±0.10	0.13±0.05[a]
HA treatment	5.54±0.06[a]	0.12±0.08[a]

(B) Effects of DOT1LsiRNA on cisplatin-induced cell growth inhibition in CD44v3^{high}ALDH1^{high} cells.

Treatments	Cisplatin-Induced Tumor Cell Growth Inhibition IC_{50} (μM)*	
	Scrambled siRNA-treated cells	DOT1L siRNA-treated cells
No treatment (control)	2.00±0.08	0.15±0.07[b]
HA treatment	5.69±0.07[b]	0.11±0.03[b]

(C) Effects of anti-miR-10b inhibitor on cisplatin-induced cell growth inhibition in CD44v3^{high}ALDH1^{high} cells.

Treatments	Cisplatin-Induced Tumor Cell Growth Inhibition IC_{50} (μM)*	
	Negative miRNA-treated cells	Anti-miR-10b inhibitor-treated cells
No treatment (control)	1.85±0.6	0.15±0.02[c]
HA treatment	5.29±0.2[c]	0.09±0.01[c]

(D) Effects of RhoC siRNA, cIAP-2 siRNA & XIAP siRNA on cisplatin-induced cell growth inhibition in CD44v3^{high}ALDH1^{high} cells.

Treatments	Cisplatin-Induced Tumor Cell Growth Inhibition IC_{50} (μM)*			
	Scrambled siRNA-treated cells	RhoC siRNA-treated cells	cIAP-2 siRNA-treated cells	XIAP siRNA-treated cells
No treatment (control)	2.20±0.10	0.14±0.02[d]	0.12±0.01[d]	0.13±0.01[d]
HA treatment	5.44±0.09[d]	0.11±0.01[d]	0.10±0.02[d]	0.09±0.02[d]

* Tumor cell growth inhibition (IC_{50}) is designated as "the micromolar concentration of chemotherapeutic drug (*e.g.* cisplatin, 24h treatment) that causes 50% inhibition of tumor cell growth" using 3-(4,5-dimethylthiazol-2-yl)-2,5-diphenyltetrazolium bromide-based growth assay as described under "Experimental Procedures." IC_{50} values are presented as the means ± S.E. (with $n = 4$). All assays consisted of at least six replicates and were performed on at least 4 different experiments.
[a] Data are statistically significant ($P < 0.001$; analysis of variance; $n = 4$) as compared with control samples (normal IgG-treated cells without HA addition).
[b,d] Data are statistically significant ($P < 0.001$; analysis of variance; $n = 4$) as compared with control samples (scrambled siRNA-treated cells without HA addition).
[c] Data are statistically significant ($P < 0.001$; analysis of variance; $n = 4$) as compared with control samples (miRNA negative control-treated cells without HA addition).

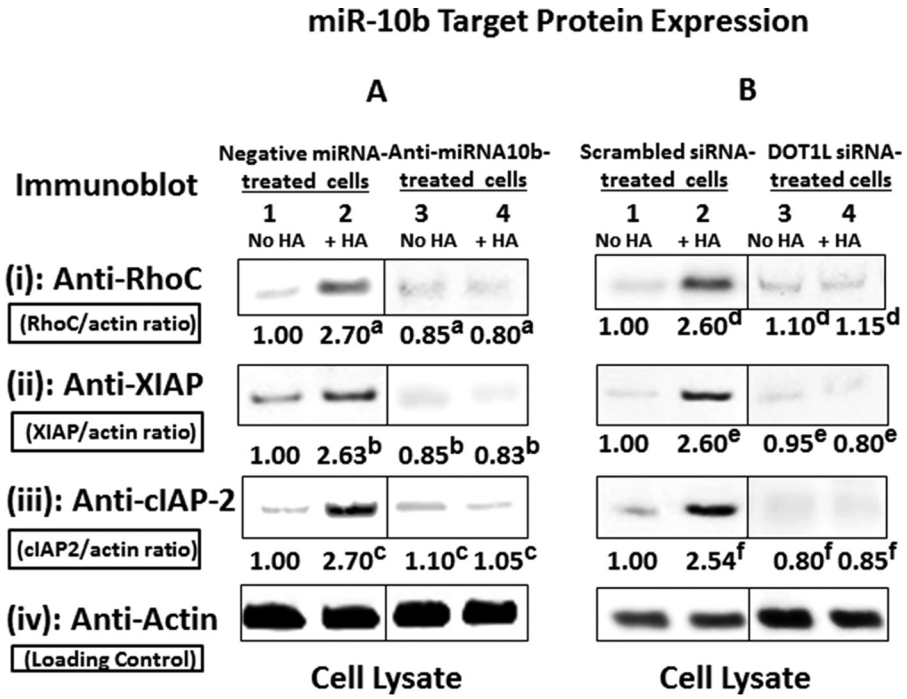

FIGURE 6. **Analyses of HA-mediated RhoC, XIAP, and cIAP-2 expression in CD44v3^{high}ALDH1^{high} cells.** *A,* detection of the expression of RhoC, XIAP, and cIAP-2 by anti-RhoC-mediated immunoblotting (*panel i*), anti-XIAP-mediated immunoblotting (*panel ii*), and anti-cIAP-2-mediated immunoblotting (*panel iii*) using cell lysate isolated from CD44v3^{high}ALDH1^{high} cells treated with negative miRNA control (treated with no HA (*lane 1*) or with HA for 24 h (*lane 2*)) or treated with anti-miR-10b inhibitor with no HA (*lane 3*) or with HA addition for 24 h (*lane 4*). The amount of actin detected by anti-actin-mediated immunoblot (*d*) in each gel lane was used as a loading control. (The ratio of RhoC (*panel i*) or XIAP (*panel ii*) or cIAP-2 (*panel iii*), and actin (*panel iv*) was determined by densitometry and normalized to the value of control (negative miRNA control with no HA-treated samples) designated as 1:00. The values expressed represent an average of triplicate determinations of four experiments with S.D. of less than 5%.) *B,* detection of the expression of RhoC, cIAP-2, and XIAP by anti-RhoC-mediated immunoblotting (*panel i*), anti-cIAP-2-mediated immunoblotting (*panel ii*), and anti-XIAP-mediated immunoblotting (*panel iii*) using cell lysate isolated from CD44v3^{high}ALDH1^{high} cells treated with scrambled siRNA (treated with no HA (*lane 1*) or with HA for 24 h (*lane 2*)) or treated with DOT1LsiRNA with no HA (*lane 3*) or with HA addition for 24 h (*lane 4*). The amount of actin detected by anti-actin-mediated immunoblot (*d*) in each gel lane was used as a loading control. (The ratio of RhoC (*panel i*) or XIAP (*panel ii*) or cIAP-2 (*panel iii*) and actin (*panel iv*) was determined by densitometry and normalized to the value of control (scrambled siRNA control with no HA-treated samples) designated as 1:00. The values expressed represent an average of triplicate determination of four experiments with S.D. of less than 5%.) ^{a,b,c}, statistically significant ($p < 0.001$; analysis of variance; $n = 4$) as compared with control samples (miRNA negative control-treated cells without HA addition). ^{d,e,f}, statistically significant ($p < 0.001$; analysis of variance; $n = 4$) as compared with control samples (scrambled siRNA-treated cells without HA addition).

lane 1, and Table 3, B). These findings support the notion that the expression of RhoC and tumor cell invasion are HA-dependent. Most importantly, down-regulation of miR-10b or DOT1L by treating cells with an anti-miR-10b inhibitor (but not negative miRNA control-treated samples) or DOT1LsiRNA (but not scrambled siRNA-treated samples) significantly attenuates the HA-activated RhoC expression (at least ~30–40% decrease in RhoC expression) (Fig. 6, *A* and *B* (*panel i*), *lanes 3* and *4 versus lanes 1* and *2*) and tumor cell invasion (at least ~40–70% reduction in tumor cell invasion) (Table 3, B and C). These findings further support the contention that HA-activated DOT1L signaling and miR-10b actively participate in the up-regulation of the cytoskeleton regulator, RhoGTPase (RhoC), and tumor cell invasion in CD44v3^{high} ALDH1^{high} cells.

Survival Protein Expression and Chemotherapy Resistance—Inhibitors of the apoptosis family of proteins (IAPs such as cIAP-2 and XIAP) are frequently up-regulated in CSCs following HA treatment (10). Importantly, high levels of IAPs in CSCs increase cell survival due to the binding of IAPs to caspases and suppressing apoptosis (27). Our data indicate that the expression of XIAP and cIAP-2 is significantly increased (at least ~2.5-fold increase) in CD44v3^{high}ALDH1^{high} cells treated with a miRNA-negative control reagent (or scrambled sequence siRNA) in the presence of HA (Fig. 6, *A* and *B*, *panels ii* and *iii*, *lane 2 versus lane 1*). In contrast, XIAP and cIAP-2 are detected in relatively low levels (at least ~40% reduction) in CD44v3^{high} ALDH1^{high} cells treated with an miRNA-negative control reagent (or scrambled sequence siRNA) with no HA (Fig. 6, *A* and *B*, *panels ii* and *iii*, *lane 1 versus lane 2*). Our data also indicate that CD44v3^{high}ALDH1^{high} cells treated with DOT1LsiRNA (but not a scrambled sequence siRNA in the presence of HA) display a decreased amount of IAP (cIAP-2 and XIAP) expression (at least ~40–70% reduction) (Fig. 6*B, panels ii* and *iii*, *lane 3* and *lane 4 versus lane 1* and *lane 2*). These observations confirm that HA-mediated DOT1L signaling is closely linked to the regulation of IAPs in CD44v3^{high}ALDH1^{high} cells. We also noted that down-regulation of miR-10b by treating CD44v3^{high}ALDH1^{high} cells with an anti-miR-10b inhibitor (but not a negative control miRNA) results in the down-regulation of IAPs (Fig. 6*A, panels ii* and *iii*, *lane 3* and *lane 4 versus lane 1* and *lane 2*) (at least ~40–70% reduction) in the presence of HA. Together, these results indicate that the signaling network consisting of DOT1L-regulated H3K79 methylation and miR-10b is functionally coupled to the stimulation of survival protein (*e.g.* cIAP-2 and XIAP) production in CSCs. These spe-

cific effects may facilitate the CSC-mediated HNSCC progression following HA treatment.

Moreover, our data indicate that the addition of HA to scrambled siRNA-treated CD44v3^{high}ALDH1^{high} cells or negative miRNA-treated CD44v3^{high}ALDH1^{high} cells significantly decreases the ability of cisplatin to induce tumor cell death (at least ~2.5-fold increase in cisplatin resistance) (Table 4, B and C). These observations strongly suggest that HA causes both a decrease in tumor cell death and an increase in tumor cell survival leading to the enhancement of chemoresistance. Moreover, down-regulation of DOT1L or miR-10b expression (by treating CD44v3^{high}ALDH1^{high} HNSCC cells with DOT1LsiRNA or transfected CD44v3^{high}ALDH1^{high} cells with an anti-miR-10b inhibitor (but not scrambled sequence siRNA or with negative miRNA control)) effectively attenuates HA-mediated anti-apoptosis/survival in CD44v3^{high}ALDH1^{high} cells (Fig. 6, *A, panels ii* and *iii, lanes 1–4,* and *B, panels ii* and *iii*, *lanes 1–4*) and enhances cisplatin sensitivity in CD44v3^{high}ALDH1^{high} cells (at least ~40–90% reduction in cisplatin-resistance) (Table 4, B and C). These findings suggest that HA-mediated cisplatin resistance in CD44v3^{high}ALDH1^{high} cells is DOT1L and miR-10b-dependent.

Further analyses indicate that down-regulation of DOT1L or miR-10 targets such as RhoC or cIAP-2 or XIAP by treating CD44v3^{high}ALDH1^{high} cells with RhoC siRNA or cIAP-2siRNA or XIAP siRNA effectively (but not scrambled siRNA-treated cells) inhibits HA-mediated tumor cell invasion (at least ~40–70% reduction in invasiveness) (Table 3, D) and increases cisplatin-induced chemosensitivity (at least ~40–90% reduction in cisplatin resistance) (Table 4, D). These findings strongly support the contention that the HA-mediated DOT1L/H3K79 methylation signaling pathways and miR-10b-regulated RhoC/cIAP-2/XIAP appear to significantly contribute to tumor cell invasion and chemosensitivity in head and neck cancer.

Discussion

Emerging evidence suggests that CSCs represent the most tumorigenic and chemoresistant cells within a heterogeneous HNSCC tumor mass (10). All stem cells are thought to exist in specialized microenvironments known as niches (28, 29). Components present in the niches can regulate stem cell behavior through direct binding to stem cell surface receptors or via indirect activation of paracrine signaling. ECM components, including HA, are known to be present in at least one of the stem cell niches (28, 29). Because CD44 is a major HA receptor, it provides a physical linkage between matrix HA and various transcription factors that regulate tumor cell functions through distinct signaling pathways (30, 42). In fact, both HA and CD44 have been shown to be involved in self-renewal and differentiation of human embryonic stem cells (31, 32). In this study, we observed that HA treatment promotes sphere formation (cell-cell adhesion), self-renewal/growth, and differentiation (*e.g.* tumor cell invasion) in highly tumorigenic CD44v3^{high}ALDH1^{high} tumor cells (Table 2). These observations support the contention that HA signaling is directly involved in the regulation of cancer stem cell properties in CD44v3^{high}ALDH1^{high} cells. A previous study showed that the expression of two CD44 isoforms (*i.e.* CD44s and CD44v6) is found in the majority of the cells in head and neck tissue and that this type of marker by itself was not able to distinguish normal from benign or malignant epithelial cells from the head and neck region (44). Our results indicated that the expression of CD44s was not significantly different in metastatic lymph nodes and primary tumors. However, the expression of several CD44 variant isoforms was associated with advanced T stage (*e.g.* CD44v3), regional (CD44v3), and distant (CD44v10) metastasis, perineural invasion (CD44v6), and radiation failure (CD44v10) (6). Both CD44v6^{high}ALDH1^{high} and CD44v10^{high}ALDH1^{high} subpopulations appear to be present as a very minor tumor cell population in HSC-3 cells based on FACTS sorting. Therefore, we are not able to examine the CSC properties of these subpopulations at this time.

Most histone H3 modifications occur on residues within the N-terminal tail. In contrast, H3K79 is located in a loop within the globular domain exposed on the nucleosome surface (19). H3K79 methylation by DOT1L (the H3K79 methyltransferase) is frequently correlated with transcriptional activity (16, 19) and cancer progression (21, 22). For example, DOT1L-regulated H3K79 methylation promotes leukemia formation induced by *MLL*-AF9 translocations (21). Treatment of *MLL*-rearranged leukemia with EPZ00477 or EPZ-5676 (potent and selective aminonucleoside inhibitors of DOT1L histone methyltransferase activity) causes cell death in acute leukemia lines bearing *MLL* translocations (33, 34). Down-regulation of H3K79 methyltransferase, DOT1L, using specific DOT1LsiRNA also reduced proliferation of lung cancer cells (22). These findings indicate that H3K79 methyltransferase, DOT1L, plays an important role in promoting cancer formation.

The recent discovery of miRNAs in CSCs has broadened the area of gene regulation implicated in tumorigenesis and CSC modulation (35, 42, 43). In this study, we observed that HA is capable of stimulating DOT1L and H3K79 methylation in CSCs. Up-regulation of DOT1L and monomethyl-H3K79 by HA may provide a unique binding surface along the chromatin fibers to stabilize the interaction between enhancers and their target promoters, thereby rendering a high level of gene transcription. Our ChIP results also indicate that monomethyl-H3K79 (and to a lesser extent trimethyl-H3K79, data not shown) is recruited to the promoter region of miR-10b (Fig. 4) resulting in miR-10 production (Fig. 5) in HA-treated CSCs. Down-regulation of DOT1L by DOT1L siRNA (but not scrambled siRNA) effectively blocks the monomethyl-H3K79-regulated miR-10b gene expression and production in these CSC-like cells (Fig. 4). These findings strongly suggest that DOT1L-regulated monomethyl-H3K79 is required for HA-activated miR-10 production in CD44v3^{high}ALDH1^{high} (CSC) cells. These findings are consistent with previous observations indicating monomethyl-H3K79 is preferentially associated with active genes (36).

Tumor invasion and metastasis are the primary causes of morbidity in patients diagnosed with solid tumors such as head and neck cancer (1). It is now certain that cytoskeletal functions are directly involved in tumor cell invasion of surrounding tissue and metastasis (37). A number of studies have aimed at

identifying those molecules that are specifically expressed by cancer stem cells and correlate with metastatic behavior. The gene networks orchestrated by many oncogenic miRNAs in CSCs are still largely unknown, although some key targets have been identified as being involved in head and neck cancer progression (10). Here, we observed that HA/CD44-activated miR-10 production plays an important role in up-regulating the cytoskeleton regulator, RhoC, in CSC-like cells. Most importantly, we observed that down-regulation of HA-activated DOT1L signaling (by DOT1L siRNA) and miR-10b production (by anti-miR-10b inhibitor) not only reduces RhoGTPase (RhoC) expression (Fig. 5) but also impairs tumor cell migration/invasion (Table 3). These findings clearly establish a causal link between DOT1L/H3K79 methylation and miR-10b function, including cytoskeleton-regulated CSC invasion.

Cisplatin is one of the most common chemotherapies used to treat head and neck cancer today. The ability of this drug to induce tumor cell death is often counteracted by the presence of anti-apoptotic regulators leading to chemoresistance (38–40). Several lines of evidence point toward the IAP family (*e.g.* cIAP-2 and XIAP) playing a major role in oncogenesis via their effective suppression of apoptosis (27). The mode of action of IAPs in suppressing apoptosis appears to be through direct inhibition of caspases and pro-caspases (primarily caspase 3 and 7) (27). IAPs also support chemoresistance directly by preventing tumor cell death induced by anticancer agents (41). Although certain anti-apoptotic proteins (*e.g.* Bcl-xL) have been shown to participate in anti-apoptosis and chemoresistance in HA/CD44-activated tumor cells, the involvement of IAPs in HA/CD44-mediated HNSCC cell survival and chemoresistance (10, 13, 42, 43) has only recently started to receive attention. In this study we demonstrated that down-regulation of HA/CD44-activated DOT1L signaling (by DOT1L siRNA) and miR-10b production (by anti-miR-10b inhibitor) inhibits the expression of survival proteins (*e.g.* cIAP-2 and XIAP) (Fig. 6). Subsequently, these signaling perturbation events contribute to apoptosis and chemosensitivity (Table 4). Most importantly, inhibition of cIAP-2 or XIAP expression (by cIAP-2 siRNA or XIAP siRNA) also enhances cisplatin-induced chemosensitivity (Table 4). These findings suggest that DOT1L- and miR-10-regulated signaling pathways and their downstream targets (*e.g.* RhoC, cIAP-2, and XIAP) may represent new targets for therapeutic agents to cause CSCs to become less invasive, undergo apoptosis/death, and not remain chemotherapy-resistant during head and neck cancer progression.

As summarized in Fig. 7, we propose that HA binding (*step 1*) to CSCs promotes DOT1L/H3K79 methylation-mediated epigenetic changes (*step 2*), resulting in H3K79 methylation binding to the E-box region of the miR-10b promoter (*step 3*), miR-10b gene expression (*step 4*), and mature miR-10b production (*step 5*). The resultant miR-10b then promotes up-regulation of RhoC (cytoskeleton activator) (Fig. 7, *step 6*) and CSC-mediated invasion. Moreover, miR-10b also induces survival protein, IAP (c-IAP-1, cIAP-2, and XIAP) expression (Fig. 7, *step 7*), HNSCC cell anti-apoptosis/survival, and chemoresistance. Taken together, these findings suggest that targeting the HA/CD44-mediated DOT1L/H3K79 methylation pathways and miR-10b function may provide new drug targets to induce cancer stem cell apoptosis/death and overcome cisplatin resistance in CSC-derived HNSCC cells.

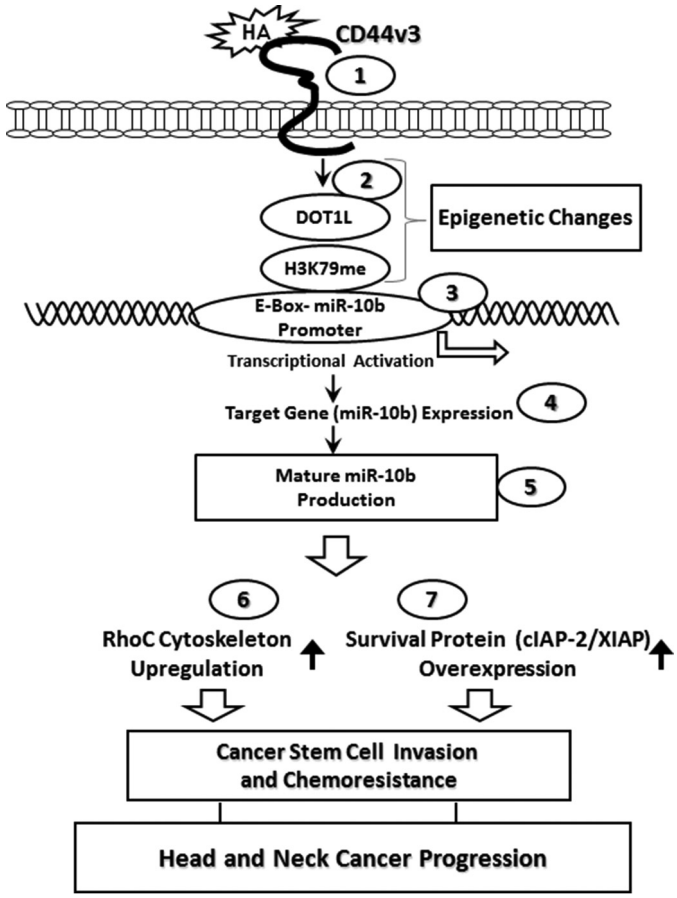

FIGURE 7. **Proposed model for HA-mediated DOT1L-H3K79 methylation signaling in the regulation of miRNA-10 production and CSC functions in CD44v3^{high}ALDH1^{high} cells.** HA binding (*step 1*) to CSCs promotes DOT1L/H3K79 methylation-mediated epigenetic changes (*step 2*), resulting in monomethyl-H3K79 binding to E-box region of miR-10b promoter (*step 3*), miR-10b gene expression (*step 4*), and mature miR-10b production (*step 5*). The resultant miR-10b then promotes up-regulation of RhoC (cytoskeleton activator) and CSC-mediated invasion (*step 6*). Moreover, miR-10b also induces survival protein IAP (cIAP-2 and XIAP) expression, HNSCC cell anti-apoptosis/survival, and chemoresistance (*step 7*). Taken together, these findings suggest that targeting HA-mediated DOT1L/H3K79 methylation pathways and miR-10b function may provide a new drug target to sensitize cancer stem cell apoptosis/death and overcome cisplatin resistance in CSC-derived HNSCC cells.

Author Contributions—L. Y. W. B., G. W., and M. S. conceived the study and analyzed the data. L. Y. W. B. wrote the paper. G. W. performed FACS and cell sorting. M. S. conducted immunoblotting analyses and transfection experiments. All authors analyzed the results and approved the final version of the manuscript.

Acknowledgment—We gratefully acknowledge the assistance of Dr. Gerard J. Bourguignon in the preparation and review of this manuscript.

References

1. Parkin, D. M., Bray, F., Ferlay, J., and Pisani, P. (2005) Global cancer statistics, 2002. *CA Cancer J. Clin.* **55,** 74–108
2. Laurent, T. C., and Fraser, J. R. (1992) Hyaluronan. *FASEB J.* **6,** 2397–2404

3. Lee, J. Y., and Spicer, A. P. (2000) Hyaluronan: a multifunctional, megadalton, stealth molecule. *Curr. Opin. Cell Biol.* **12,** 581–586
4. Underhill, C. (1992) CD44: the hyaluronan receptor. *J. Cell Sci.* **103,** 293–298
5. Toole, B. P., and Hascall, V. C. (2002) Hyaluronan and tumor growth. *Am. J. Pathol.* **161,** 745–747
6. Wang, S. J., Wong, G., de Heer, A. M., Xia, W., and Bourguignon, L. Y. (2009) CD44 variant isoforms in head and neck squamous cell carcinoma progression. *Laryngoscope* **119,** 1518–1530
7. Wang, S. J., and Bourguignon, L. Y. (2011) Role of hyaluronan-mediated CD44 signaling in head and neck cell carcinoma progression and chemoresistance. *Am J. Pathol.* **178,** 956–963
8. Screaton, G. R., Bell, M. V., Jackson, D. G., Cornelis, F. B., Gerth, U., and Bell, J. I. (1992) Genomic structure of DNA coding the lymphocyte homing receptor CD44 reveals 12 alternatively spliced exons. *Proc. Natl. Acad. Sci. U.S.A.* **89,** 12160–12164
9. Bourguignon, L. Y., Earle, C., Wong, G., Spevak, C. C., and Krueger, K. (2012) Stem cell marker (Nanog) and Stat-3 signaling promotes MicroRNA-21 expression and chemoresistance in hyaluronan/CD44-activated head and neck squamous cell carcinoma cells. *Oncogene* **31,** 149–160
10. Bourguignon, L. Y., Wong, G., Earle, C., and Chen, L. (2012) Hyaluronan-CD44v3 interaction with Oct4-Sox2-Nanog promotes miR-302 expression leading to self-renewal, clone formation and cisplatin resistance in cancer stem cells from head and neck squamous cell carcinoma. *J. Biol. Chem.* **287,** 32800–32824
11. Chang, S. S., Jiang, W. W., Smith, I., Poeta, L. M., Begum, S., Glazer, C., Shan, S., Westra, W., Sidransky, D., and Califano, J. A. (2008) MicroRNA alterations in head and neck squamous cell carcinoma. *Int. J. Cancer* **123,** 2791–2797
12. Volinia, S., Calin, G. A., Liu, C. G., Ambs, S., Cimmino, A., Petrocca, F., Visone, R., Iorio, M., Roldo, C., Ferracin, M., Prueitt, R. L., Yanaihara, N., Lanza, G., Scarpa, A., Vecchione, A., *et al.* (2006) A microRNA expression signature of human solid tumors defines cancer gene targets. *Proc. Natl. Acad. Sci. U.S.A.* **103,** 2257–2261
13. Bourguignon, L. Y., Xia, W., and Wong, G. (2009) Hyaluronan-mediated CD44 interaction with p300 and SIRT1 regulates β-catenin signaling and NFκB-specific transcription activity leading to MDR1 and Bcl-xL gene expression and chemoresistance in breast tumor cells. *J. Biol. Chem.* **284,** 2657–2671
14. Ma, L., Teruya-Feldstein, J., and Weinberg, R. A. (2007) Tumour invasion and metastasis initiated by microRNA-10b in breast cancer. *Nature* **449,** 682–688
15. Bourguignon, L. Y., Wong, G., Earle, C., Krueger, K., and Spevak, C. (2010) Hyaluronan-CD44 interaction promotes c-Src-mediated twist signaling, microRNA-10b expression, and RhoA/RhoC up-regulation, leading to Rho-kinase-associated cytoskeleton activation and breast tumor cell invasion. *J. Biol. Chem.* **285,** 36721–36735
16. Shilatifard, A. (2006) Chromatin modifications by methylation and ubiquitination: Implications in the regulation of gene expression. *Annu. Rev. Biochem.* **75,** 243–269
17. Ng, H. H., Feng, Q., Wang, H., Erdjument-Bromage, H., Tempst, P., Zhang, Y., and Struhl, K. (2002) Lysine methylation within the globular domain of histone H3 by Dot1 is important for telomeric silencing and Sir protein association. *Genes Dev.* **16,** 1518–1527
18. van Leeuwen, F., Gafken, P. R., Gottschling, D. E. (2002) Dot1p modulates silencing in yeast by methylation of the nucleosome core. *Cell* **109,** 745–756
19. Feng, Q., Wang, H., Ng, H. H., Erdjument-Bromage, H., Tempst, P., Struhl, K., and Zhang, Y. (2002) Methylation of H3-lysine 79 is mediated by a new family of HMTases without a SET domain. *Curr. Biol.* **12,** 1052–1058
20. San-Segundo, P. A., and Roeder, G. S. (2000) Role for the silencing protein Dot1 in meiotic checkpoint control. *Mol. Biol. Cell* **11,** 3601–3615
21. Bernt, K. M., Zhu, N., Sinha, A. U., Vempati, S., Faber, J., Krivtsov, A. V., Feng, Z., Punt, N., Daigle, A., Bullinger, L., Pollock, R. M., Richon, V. M., Kung, A. L., and Armstrong, S. A. (2011) MLL-rearranged leukemia is dependent on aberrant H3K79 methylation by DOT1L. *Cancer Cell* **20,** 66–78
22. Kim, W., Kim, R., Park, G., Park, J. W., and Kim, J. E. (2012) Deficiency of H3K79 histone methyltransferase Dot1-like protein (DOT1L) inhibits cell proliferation. *J. Biol. Chem.* **287,** 5588–5599
23. Janzen, C. J., Hake, S. B., Lowell, J. E., and Cross, G. A. (2006) Selective di- or trimethylation of histone H3 Lysine 76 by two DOT1 homologs is important for cell cycle regulation in *Trypanosoma brucei*. *Mol. Cell* **23,** 497–507
24. Chen, Y. C., Chen, Y. W., Hsu, H. S., Tseng, L. M., Huang, P. I., Lu, K. H., Chen, D. T., Tai, L. K., Yung, M. C., Chang, S. C., Ku, H. H., Chiou, S. H., and Lo, W. L. (2009) Aldehyde dehydrogenase 1 is a putative marker for cancer stem cells in head and neck squamous cancer. *Biochem. Biophys. Res. Commun.* **385,** 307–313
25. Clay, M. R., Tabor, M., Owen, J. H., Carey, T. E., Bradford, C. R., Wolf, G. T., Wicha, M. S., and Prince, M. E. (2010) Single-marker identification of head and neck squamous cell carcinoma cancer stem cells with aldehyde dehydrogenase. *Head Neck* **32,** 1195–1201
26. Guessous, F., Alvarado-Velez M., Marcinkiewicz, L., Zhang, Y., Kim, J., Heister, S., Kefas, B., Godlewski, J., Schiff, D., Purow, B., and Abounader, R. (2013) Oncogenic effects of miR-10b in glioblastoma stem cells. *J. Neurooncol.* **112,** 153–163
27. Hunter, A. M., LaCasse, E. C., and Korneluk, R. G. (2007) The inhibitors of apoptosis (IAPs) as cancer targets. *Apoptosis* **12,** 1543–1568
28. Haylock, D. N., and Nilsson, S. K. (2006) The role of hyaluronic acid in hemopoietic stem cell biology. *Regen. Med.* **1,** 437–445
29. Astachov, L., Vago, R., Aviv, M., and Nevo, Z. (2011) Hyaluronan and mesenchymal stem cells: from germ layer to cartilage and bone. *Front. Biosci.* **16,** 261–276
30. Bourguignon, L. Y. (2012) Hyaluronan-CD44 interaction promotes microRNA signaling and RhoGTPase activation leading to tumor progression. *Small GTPases* **3,** 53–59
31. Wheatley, S. C., and Isacke, C. M. (1995) Induction of a hyaluronan receptor, CD44, during embryonal carcinoma and embryonic stem cell differentiation. *Cell Adhes. Commun.* **3,** 217–230
32. Choudhary, M., Zhang, X., Stojkovic, P., Hyslop, L., Anyfantis, G., Herbert, M., Murdoch, A. P., Stojkovic, M., and Lako, M. (2007) Stem cells. Putative role of hyaluronan and its related genes, HAS2 and RHAMM, in human early preimplantation embryogenesis and embryonic stem cell characterization. *Stem Cells* **25,** 3045–3057
33. Daigle, S. R., Olhava, E. J., Therkelsen, C. A., Majer, C. R., Sneeringer, C. J., Song, J., Johnston, L. D., Scott, M. P., Smith, J. J., Xiao, Y., Jin, L., Kuntz, K. W., Chesworth, R., Moyer, M. P., Bernt, K. M., *et al.* (2011) Selective killing of mixed lineage leukemia cells by a potent small-molecule DOT1L inhibitor. *Cancer Cell* **20,** 53–65
34. Daigle, S. R., Olhava, E. J., Therkelsen, C. A., Basavapathruni, A., Jin, L., Boriack-Sjodin, P. A., Allain, C. J., Klaus, C. R., Raimondi, A., Scott, M. P., Waters, N. J., Chesworth, R., Moyer, M. P., Copeland, R. A., Richon, V. M., and Pollock, R. M. (2013) Potent inhibition of DOT1L as treatment of MLL-fusion leukemia. *Blood* **122,** 1017–1025
35. Sun, X., Jiao, X., Pestell, T. G., Fan, C., Qin, S., Mirabelli, E., Ren, H., and Pestell, R. G. (2014) MicroRNAs and cancer stem cells: the sword and the shield. *Oncogene* **33,** 4967–4977
36. Barski, A., Cuddapah, S., Cui, K., Roh, T. Y, Schones, D. E., Wang, Z., Wei, G., Chepelev, I., and Zhao, K. (2007) High-resolution profiling of histone methylations in the human genome. *Cell* **129,**823–837
37. Seton-Rogers, S. (2009) Tumour suppressors: different roads to inactivation. *Nat. Rev. Cancer* **9,** 610–611
38. Shiga, H., Rasmussen, A. A., Johnston, P. G., Langmacher, M., Baylor, A., Lee, M., and Cullen, K. J. (2000) Prognostic value of c-erbB2 and other markers in patients treated with chemotherapy for recurrent head and neck cancer. *Head Neck* **22,** 599–608
39. Kato, T., Duffey, D. C., Ondrey, F. G., Dong, G., Chen, Z., Cook, J. A., Mitchell, J. B., and Van Waes, C. (2000) Cisplatin and radiation sensitivity in human head and neck squamous carcinomas are independently modulated by glutathione and transcription factor NF-κB. *Head Neck* **22,** 748–759
40. Bradford, C. R., Zhu, S., Ogawa, H., Ogawa, T., Ubell, M., Narayan, A., Johnson, G., Wolf, G. T., Fisher, S. G., and Carey, T. E. (2003) p53 mutation

correlates with cisplatin sensitivity in head and neck squamous cell carcinoma lines. *Head Neck* **25,**654–661

41. Gyrd-Hansen, M., and Meier, P. (2010) IAPs: from caspase inhibitors to modulators of NF-κB, inflammation and cancer. *Nat. Rev. Cancer* **10,** 561–574
42. Bourguignon, L. Y., Shiina, M., and Li, J. J. (2014) Hyaluronan-CD44 interaction promotes oncogenic signaling and microRNA functions in cancer stem cells leading to tumor progression. *Adv. Cancer Res.* **123,** 255–275
43. Shiina, M., and Bourguignon, L. Y. (2015) Selective activation of cancer stem cells by size-specific hyaluronan in head and neck cancer. *Int. J. Cell Biol.* **2015,** 989070
44. Mack, B., and Gires, O. (2008) CD44s and CD44v6 expression in head and neck epithelia. *PLoS ONE* **3,** e3360